Raman spectra of a rotator hindered by fields of cubic symmetry*

Hans U. Beyeler†
Department of Physics, University of Utah, Salt Lake City, Utah 84112
(Received 30 October 1973)

Raman spectra of a vibrating rotator are computed for a variety of hindering fields of cubic symmetry. Results are displayed for three types of hindering potentials localizing the rotator gradually in ⟨100⟩-, ⟨110⟩-, or ⟨111⟩-oriented minimum wells, respectively. For strong hindering potentials the spectra merge into those derived from the appropriate "tunneling model."

INTRODUCTION

Molecular-crystal defects exhibiting hindered rotation have some unique features which make their experimental investigation particularly interesting. In these systems states close to or even above the rotational barrier may be excited already at relatively low temperatures. Such excited states may thus be studied by infrared and Raman spectroscopy and give more information about the defect-lattice interaction potential than can be obtained spectroscopically from defects completely locked into a minimal-energy direction. In addition to paraelasticity and paraelectricity, such defects exhibit quantum effects due to the presence of appreciably split tunneling levels, e.g., paraelectric resonance or spectral change of the vibrational absorption under external elastic and electric fields.

To describe this type of defect a multilevel model such as the "hindered rotator" is clearly more adequate than a "tight-well model" based on weakly coupled ground states localized in the minimum wells of the potential. Detection of a "tunneling splitting" in the low-temperature vibrational absportion of CN^- in KCl[1] together with earlier results on this system[2] motivated an extended computation of hindered-rotator energy levels[3] and infrared spectra.[4] Recently Peascoe and Klein[5] performed a series of Raman experiments on OH^- in various host lattices which yielded a great amount of new data on the OH^- center. Their results and earlier Raman experiments on CN^-[6] stimulated the extension of the computations to synthetic hindered-rotator Raman spectra. Raman experiments may not only complement the infrared-absorption data on these systems but also make the great amount of homonuclear defects accessible to spectroscopic investigation.

The expanded computational model enables the study of the relation between the infrared and Raman response of a defect and its hindering potential for a large manifold of cubic potentials. It is the purpose of this publication to display a few Raman spectra resulting from frequently discussed hindering potentials.

HINDERED-ROTATOR MODEL

The model underlying the computations is that of a vibrating rotator whose wave function can be expressed as

$$\psi_{tot} = \psi_{vibr}(R)\,\psi_{rot}(\phi, \theta)\,\psi', \tag{1}$$

with R being the internuclear coordinate measured from equilibrium distance, ϕ and θ are the orientational coordinates of the rotator axis. ψ' is the remaining nuclear and electronic wave function not depending on R, ϕ, or θ. Under this assumption of independent vibration and rotation both movements give additive contributions to the total energy of the system. The infrared transition matrix elements between the vibrational-rotational states are a product of a vibrational and a rotational matrix element.[7] If such a rotator is placed into a hindering potential in a first approximation only the rotational movement is affected so that only the rotational energies and transition elements are modified. On this basis the energy levels[3] and the infrared spectrum[4] of a hindered rotator have been computed. In this work Raman spectra have been computed in an analogous way using the fact that the Raman transition elements too can be factorized into a vibrational and a rotational part.

RAMAN TRANSITION MATRIX ELEMENTS AND SELECTION RULES

The matrix element relevant for dipolar nonresonant Raman transitions is that of the polarizability α_{ij} of the rotator. In the reference frame of the rotator α_{ij} is diagonal with two independent components, both depending on R, the vibrational coordinate:

TABLE I. Selection rules for E_g and T_{2g} Raman transitions between states of cubic symmetry.

	E_g					T_{2g}				
	A_1	A_2	E	T_1	T_2	A_1	A_2	E	T_1	T_2
A_1			·			A_1				·
A_2			·			A_2			·	
E	·	·	·			E			·	·
T_1				·	·	T_1	·	·	·	·
T_2				·	·	T_2	·		·	·	·

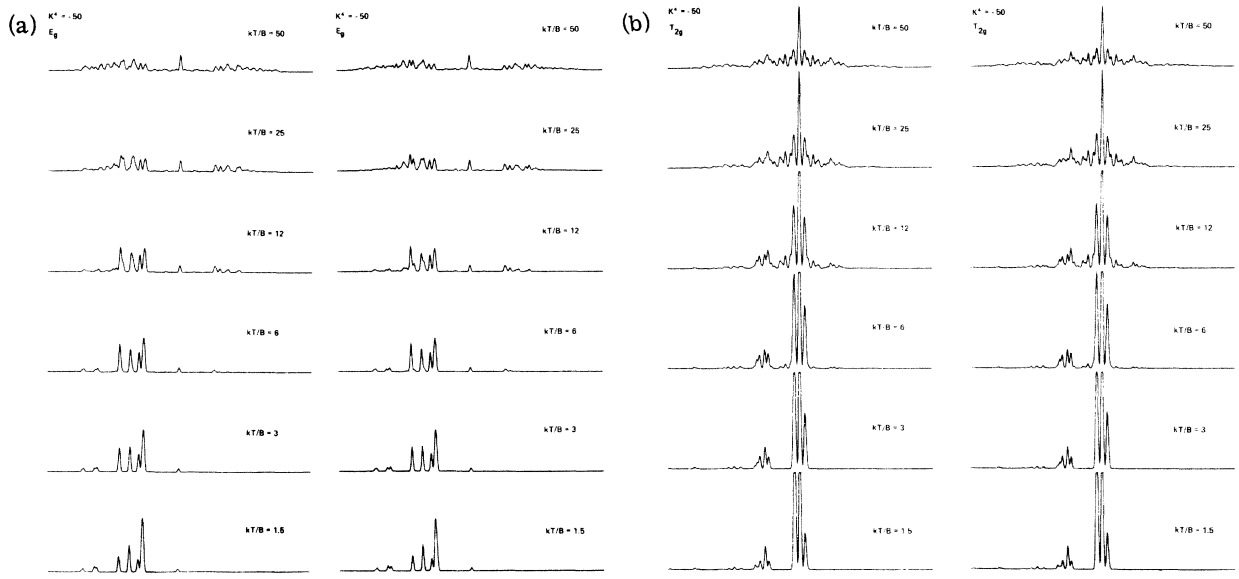

FIG. 1. Accuracy test: E_g and T_{2g} spectra for the Devonshire potential with $K^4 = -50$. (a) and (b) Left: computed with rotator states up to $l = 10$; (a) and (b) right: with rotator states up to $l = 12$.

$$\alpha^r_{ij}(R) = \begin{pmatrix} \alpha^r_{11}(R) & & \\ & \alpha^r_{11}(R) & \\ & & \alpha^r_{33}(R) \end{pmatrix}. \tag{2}$$

In the reference frame of the host crystal the polarizability is

$$\underline{\alpha}(R, \phi, \theta) = \underline{U}(\phi, \theta)\underline{\alpha}^r(R)\underline{U}^\dagger(\phi, \theta), \tag{3}$$

$\underline{U}$ is the matrix rotating the frame from the rotator to the crystal. As we limit ourselves to host crystals of cubic symmetry, $\underline{\alpha}$ has only three independent components, transforming as the representations A_{1g}, E_g, and T_{2g} of the cubic group O_h. In order to be consistent to be with Ref. 5 we use the following unnormalized expressions for the three components:

$$\begin{aligned} \alpha_{A_{1g}} &= \tfrac{1}{3}\alpha_{ii} = \tfrac{1}{3}(2\alpha^r_{11} + \alpha^r_{33}), \\ \alpha_{E_g} &= \tfrac{1}{2}(\alpha_{11} - \alpha_{22}) = \tfrac{1}{2}(\alpha^r_{33} - \alpha^r_{11})\sin^2\theta\cos 2\phi, \\ \alpha_{T_{2g}} &= \alpha_{12} = \tfrac{1}{2}(\alpha^r_{33} - \alpha^r_{11})\sin^2\theta\sin 2\theta . \end{aligned} \tag{4}$$

All three components are of the form

$$\alpha = \alpha_{\text{vibr}}(R)\alpha_{\text{rot}}(\phi, \theta). \tag{5}$$

The vibrational components may in first order assumed to be

$$\alpha_{11} = \alpha^0_{11} + \alpha'_{11}R, \quad \alpha_{22} = \alpha^0_{22} + \alpha'_{22}R. \tag{6}$$

The constant terms determine the strength of the pure rotational transitions, the linear terms that of the vibration-rotation transition. Computing the rotational matrix elements therefore yields simultaneously the fine structure of the pure rotational and that of the vibration-rotation spectrum. The relative integrated intensity of both spectra is governed by the values of the constants in Eq. (6). We further only consider rotation-vibration spectra, the pure rotational spectrum can easily be derived from the presented results.

The A_{1g} polarizability does not depend on ϕ and θ, hence A_{1g} transitions occur only between identical rotational states and are independent of the hindering potential. In the vibration-rotation spectrum they appear as a Q branch at the pure vibrational frequency. We do not further discuss these transitions as within our model they give no information about the hindering potential. (They are, however, important for the study of the interaction between rotation and vibration in a more involved model taking into account the slight dependence of the rotational constant on the vibrational state.)

Due to the even parity of the polarizability all Raman transitions only occur between states of identical parity; the additional selection rules for the E_g and T_{2g} transitions between states of cubic symmetry are displayed in Table I.

OUTLINE OF THE COMPUTATION

The computation of the energy levels, wave function, and thermal populations have been de-

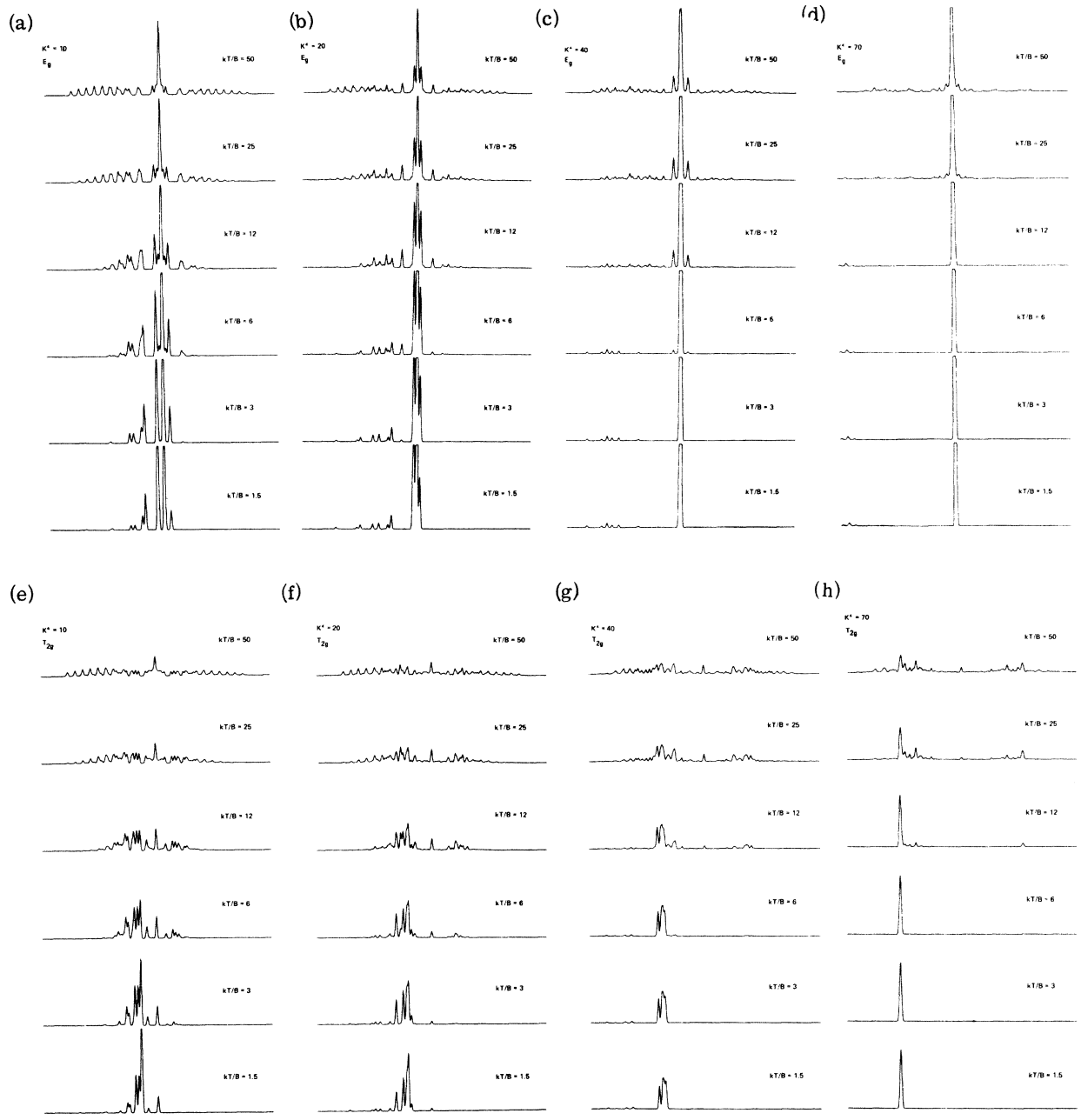

FIG. 2. Raman spectra for the Devonshire model with $K^4 = 10$, 20, 40, 70, and six temperatures expressed by the ratio kT/B.

scribed elsewhere.[3,4] The E_g and T_{2g} Raman transition matrix elements [Eq. (4)] between the free-rotator states expressed in cubic harmonics have been computed by numerical integration. The temperature-dependent intensities follow then straightforwardly. To generate the spectral plot each transition has been assigned a Gaussian line with a full width at half-height of 0.9 B. This arbitrary linewidth gives over-all satisfactory details of the spectra. The only accuracy-limiting approximation made in the calculations is the cut off in the basic set of wave functions beyond those of orbital index $l = 12$. The over-all accuracy is illustrated in Fig. 1, where for a given potential the E_g spectrum as computed with functions up to $l = 12$ is compared to that computed with functions up to $l = 10$. The temperatures and potential strengths for which results are displayed are such that the

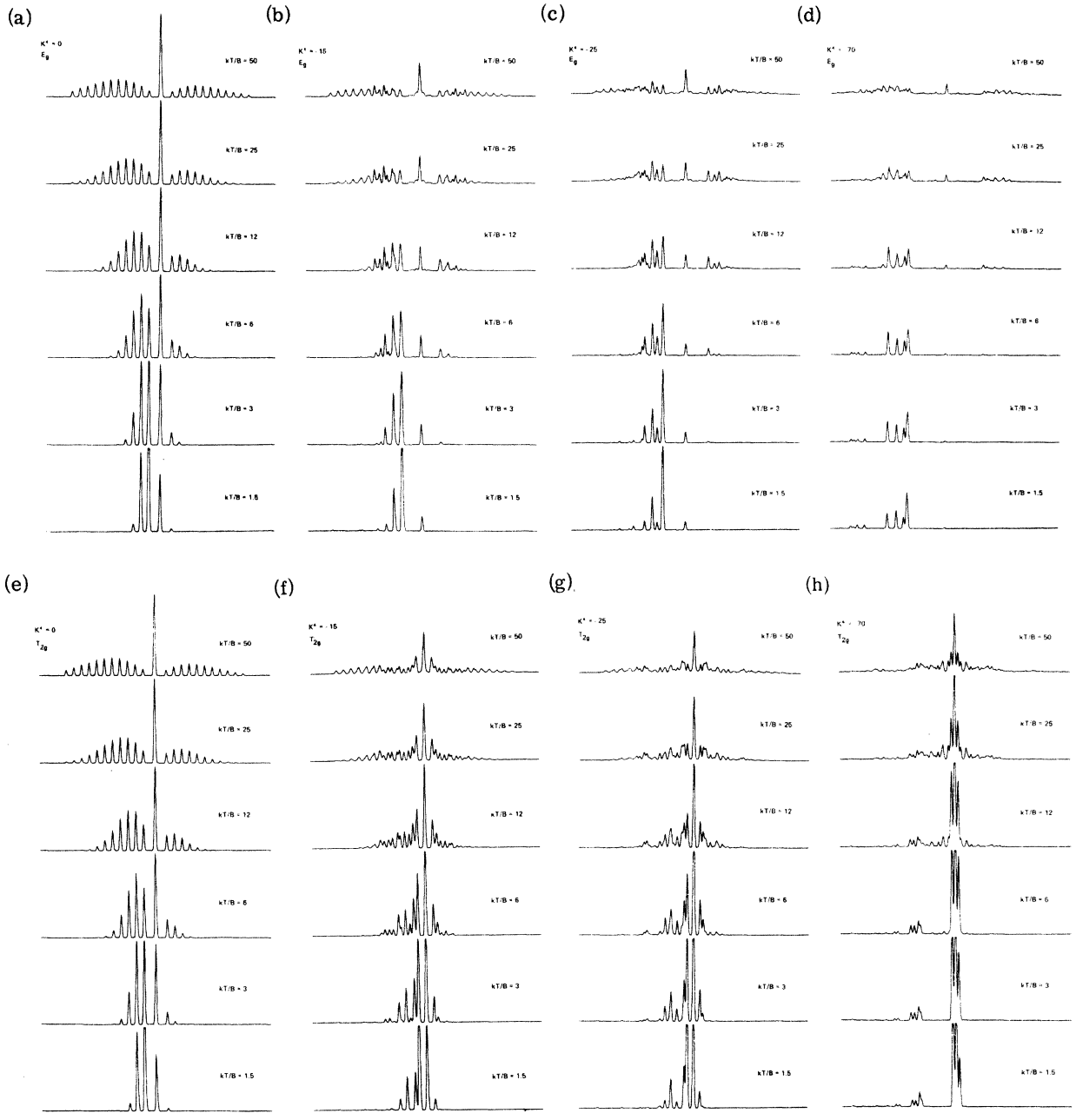

FIG. 3. Raman spectra for the Devonshire model with $K=0$, -15, -25, and -70.

inaccuracies are negligible. The computations were performed on the Univac 1108 Computer of the University of Utah.

RESULTS

The computer program is able to compute the Raman spectra of a rotator hindered by any cubic potential which can be described as a linear combination of the cubic invariant functions of order 4, 6, 8, and 10:

$$P = K^4V^4 + K^6V^6 + K^8V^8 + K^{10}V^{10}. \quad (7)$$

For the definition of the V^i see Ref. 3. Within this four-parameter manifold the relation between hindering potential and Raman spectra can be studied for a great variety of physical situations. It is beyond the scope of this publication to display more than a few results on potentials often referred to in the interpretation of experimental results. Spectra are shown for three different potentials

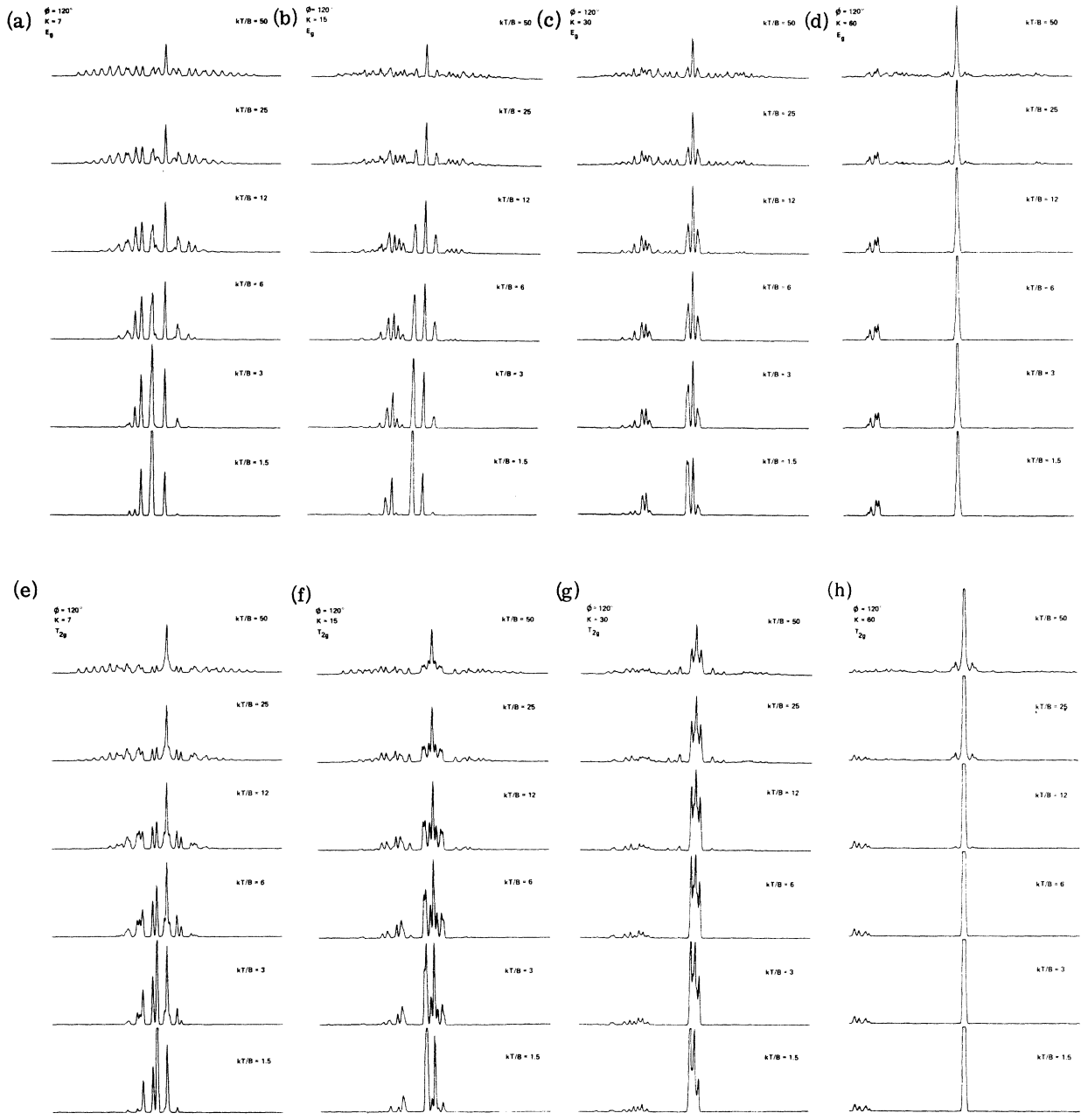

FIG. 4. Raman spectra for the hindering potential $K(V^4\cos 120° + V^6 \sin 120°)$ for $K=7$, 15, 30, and 60. This potential has minimum wells along the ⟨110⟩ axes.

which with increasing strength gradually localize the rotator in ⟨100⟩, ⟨110⟩, or ⟨111⟩ minimum wells, respectively.

Figure 2 give the E_g and T_{2g} spectra for a rotator hindered by the "Devonshire potential," $P=K^4V^4$ for four positive values of K^4 (localization in ⟨100⟩ wells). In Fig. 3 spectra are shown for the free rotator and three negative values of K^4 (localization in ⟨111⟩ wells). To get a potential with ⟨110⟩ minimum wells, combinations of V^4 and V^6 have to be considered. $P=K\,(V^4\cos 120° + V^6 \sin 120°)$ has been chosen to display gradual localization in ⟨110⟩ wells. In Fig. 4 the spectra to this potential are given for four values of K. All spectra are shown for six different values of kT/B, the temperature measured in units of the rotational constant. In conjunction with the energy levels in Ref. 3 the librational sidebands can be identified as they grad-

TABLE II. Symmetries of Raman transitions between low-lying localized states.

	⟨100⟩	⟨110⟩	⟨111⟩
Ground state–first librational state	T_{2g}	E_g, T_{2g}[a]	E_g, T_{2g}
Ground state–ground state	E_g	E_g, T_{2g}	T_{2g}

[a] E_g for libration in the (001) plane, T_{2g} for libration in the $(1\bar{1}0)$ plane.

ually emerge with increasing potential strength from the P and R branches. The symmetries of the transitions between the low-lying localized states are given in Ref. 5 and are summarized in Table II. Inspection of the spectra shows consistency between the spectra of a strongly hindered rotator and that derived from the appropriate tight-well model.

CONCLUSION

A computational model yields Raman spectra for various types of hindered rotators. The presented results display the gradual and continuous change from a free-rotator spectrum to that of a librator locked into a minimum well. Data on other than the presented hindering potentials as well as numerical results on matrix elements and wave functions can be obtained from the author. With minor changes the computation can be extended to homonuclear rotators where the multiplicity of the g and u states are determined by the nuclear spins.

*Supported in part by NSF Grant No. GH3370 4X.
†Supported by a Fellowship from the Swiss National Science Foundation. Present address: Brown Boveri Research Center, CH-5401 Baden, Switzerland.

[1]F. Lüty, Bull. Am. Phys. Soc. 18, 304 (1973). F. Lüty (unpublished).
[2]V. Narayanamurti and R. O. Pohl, Rev. Mod. Phys. 42, 201 (1970).
[3]H. U. Beyeler, Phys. Status Solidi B 52, 419 (1972).
[4]H. U. Beyeler, J. Chem. Phys. (to be published).
[5]J. G. Peascoe, thesis (University of Illinois, Urbana, 1973) (unpublished); J. G. Peascoe and M. V. Klein, J. Chem. Phys. 59, 2394 (1973).
[6]R. Callender and P. S. Pershan, Phys. Rev. Lett. 23, 947 (1969); Phys. Rev. A 2, 672 (1970).
[7]G. Herzberg, *Spectra of Diatomic Molecules*, 2nd ed. (Van Nostrand, Princeton, N. J., 1966).